J|A|C|S COMMUNICATIONS

Published on Web 01/22/2010

Indirect Detection of Labile Solute Proton Spectra via the Water Signal Using Frequency-Labeled Exchange (FLEX) Transfer

Joshua I. Friedman,[†] Michael T. McMahon,[‡] James T. Stivers,[†] and Peter C. M. Van Zijl*[,§]

Department of Pharmacology and Molecular Sciences, Johns Hopkins University School of Medicine, 725 North Wolfe Street, Baltimore, Maryland 21201, Department of Radiology and Radiological Sciences, Johns Hopkins University School of Medicine, 720 Rutland Avenue, Baltimore, Maryland 21205, and Hugo Moser Research Institute at Kennedy Krieger, F. M. Kirby Research Center, 707 North Broadway, Baltimore, Maryland 21205

Received October 22, 2009; E-mail: pvanzijl@mri.jhu.edu

Exchangeable protons have played an invaluable role in NMR studies of protein and nucleic acid structure and dynamics.[1–3] Detection of such solute (s) protons is governed by the "slow exchange" condition, where the frequency difference between solute and water (w) protons, $\Delta\omega_{sw}$, is larger than the exchange rate, k_s. However, the broad resonances of such protons are often "invisible" because they are either obscured by larger and narrower signals of other protons or hidden in the noise. We report an "exchange-rate-filtered" approach that allows the detection of such protons without interference from nonexchanging protons. Also, the transfer of these protons to water is exploited to achieve a sensitivity enhancement of several orders of magnitude with respect to standard spectroscopy. This new frequency-labeled exchange (FLEX) transfer principle is applied to detect previously "invisible" protons of some nucleic acids and peptides as well as rapidly exchanging protons ($k_s > 300\ s^{-1}$) in so-called chemical exchange saturation transfer (CEST) magnetic resonance imaging (MRI) contrast agents.[4–7] Through the FLEX approach, this latter detection can be achieved without the need for either proton saturation or additional post-processing to separate the agent signals from background signals due to direct water saturation or interfering slower magnetization-transfer effects.

The basic FLEX pulse sequence (Figure 1) consists of a series of label-transfer modules (LTMs) in which exchangeable solute protons are frequency-labeled and subsequently transferred to water. We use the general term "label" because frequency is not the only encoding type that can be used; other examples include dephasing or inversion. Here we employ binomial frequency labeling using a pair of selective $90_x/90_{-x}$ radiofrequency (RF) pulses in which the chemical shift evolution of the exchangeable protons during the period, t_{evol}, is followed by storage of the frequency information in the form of longitudinal magnetization. Subsequently, a waiting period, t_{exch}, is applied to allow exchange transfer to the solvent, where labeled protons are stored longer-term as water protons. This is a favorable situation because the water longitudinal relaxation time is fairly long ($T_{1w} \approx 1-4$ s) and the water proton pool is so large that the probability of a labeled proton going back to the solute (μM to mM concentration) is small. Signal amplification occurs because fresh z magnetization is present for the solute protons at the start of each LTM, allowing multiple opportunities to transfer labeled protons to the solvent during application of multiple (n) modules during the preparation time, t_{prep}. The sensitivity enhancement factor for this process, η, is given by

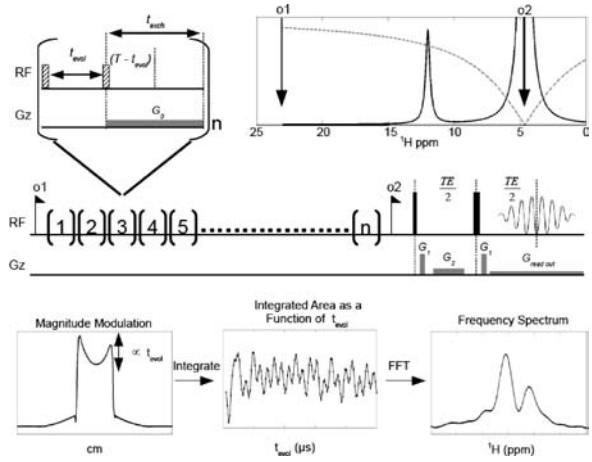

Figure 1. Frequency-labeled exchange (FLEX) transfer detection of labile protons. A series of n label transfer modules (LTMs) is applied, each containing periods for chemical shift evolution of transverse magnetization (t_{evol}) and exchange transfer of longitudinal magnetization (t_{exch}). The evolution time is varied for frequency encoding, here using a constant-time (T) approach. Short 90° pulses (small hatched rectangles, 50−100 μs) at an offset (o1) are used to selectively excite solute protons. t_{exch} should be sufficiently long for most protons to exchange even at the longest t_{evol}. To avoid radiation damping, a gradient G_0 is applied during t_{exch} and the signal is acquired using a readout gradient, providing a projection of the sample in distance units. The magnitude of this projection is modulated as a function of evolution time through exchange transfer, which can be reconstructed as a free-induction decay (FID) of amplitude PTR_s containing the signal of the exchangeable protons. A Fourier transform provides the spectrum.

$$\eta = \sum_{i=1}^{n} e^{[-1+(i-1)/n]t_{prep}/T_{1w}} \qquad (1)$$

reflecting the fact that magnetization transferred in the first LTM experiences T_{1w} decay over the full t_{prep} while that transferred in the nth module hardly relaxes. In practice, the enhancement is less because exchange during t_{exch} need not be complete and label may be lost as a result of incomplete excitation. Correcting for this with efficiency factors for exchange transfer and labeling, $\beta_s = [1 - \exp(-k_s t_{exch})]$ and λ_s, respectively, leads to the following expressions for the proton transfer ratio, PTR_s, and the effective enhancement factor, PTE_s:

$$PTR_s = \frac{[H]_s}{[H]_w} PTE_s \qquad PTE_s = \eta\beta_s\lambda_s \qquad (2)$$

in which [H] is the proton concentration. The factor λ_s depends on the excitation profile for a pair of rectangular 90° pulses of limited

[†] Department of Pharmacology & Molecular Sciences, Johns Hopkins University School of Medicine.
[‡] Department of Radiology and Radiological Sciences, Johns Hopkins University School of Medicine.
[§] Hugo Moser Research Institute at Kennedy Krieger.

bandwidth, which is shaped as a function of $\Delta\omega_{so1}$, the frequency difference between the transmitter offset of the RF pulses and the solute protons. The profile of such an excitation can be measured or calculated (see the Supporting Information) and the result squared to obtain λ_s.

In contrast to a CEST experiment, where solute protons are continuously saturated and transferred to water, no RF saturation is used in FLEX transfer; instead, an amount of signal loss is transferred that depends on the length of chemical shift evolution during t_{evol}. With the signal loss after a $\pi/2$ evolution defined as S_{av} and the original water intensity as S_0, the water signal loss at a certain t_{evol} is given by

$$I_{w,s}(t_{evol}) = PTR_s \cos(\Delta\omega_{so1} t_{evol}) = \left(1 - \frac{S_{av,s}}{S_0}\right) \cos(\Delta\omega_{so1} t_{evol}) \quad (3)$$

The water attenuation includes the effect of exchangeable protons of all solutes, and the first intuitive interpretation would be that specificity should be lost because all of the labeled protons should end up resonating at the water frequency. The strength of FLEX is that extraction of the individual frequency information for a given exchanging proton can be achieved by performing the labeling as a function of t_{evol}. This causes a magnitude modulation of the water signal that depends on the frequencies of all of the labeled exchangeable solute protons. In contrast to conventional multidimensional NMR spectroscopy,[8] however, a large sensitivity enhancement and detection through water are achieved, allowing the use of this technology for imaging of low-concentration solutes. Substituting, for convenience, $t_{evol} = t$ gives the resulting total time domain signal effect as

$$I_{w,tot}(t) = \sum_s PTR_s \, e^{-(k_s + 1/T^*_{2s})t} \frac{1}{2}(e^{i\Delta\omega_{so1}t} + e^{-i\Delta\omega_{so1}t}) \quad (4)$$

Signal decay during t_{evol} is taken into account by including the effects of exchange and effective transverse relaxation (T^*_{2s}). The frequency information for the different protons can be extracted either by using time-domain fitting or applying a Fourier transform (see the Supporting Information). Equations 2−4 also illustrate an interesting advantage of FLEX with respect to standard NMR spectroscopy, namely, that the signal includes an internal concentration reference, the directly observed water signal (an ~110 M proton pool). However, it has the practical disadvantage of detecting a very large signal with a coil optimized for measuring small induction currents. The main complication is radiation damping, in which the field induced in the coil by the large transverse water magnetization quickly drives the system back to equilibrium, resulting in an apparent decrease of T_{1w}. One way to reduce damping is to dephase the water magnetization when it is not being detected, which can be done using magnetic field gradients. These are applied during all pulse sequence periods where water evolution occurs or spurious residual transverse water magnetization may be present. Importantly, water signal acquisition should be done using a gradient-recalled echo. When this is done, the water signal is measured in the shape of a projection of the sample, which is subsequently integrated to detect the magnitude modulation. Additionally, damping can be reduced by avoiding water excitation, which was achieved through the selective excitation used for the frequency-labeling part of the sequence (50−100 μs hard pulses). One may wonder why we did not use a more selective pulse (>1 ms) centered around the protons of interest, which would have a steeper profile and allow a smaller sweep width. The reason is that using such a pulse would be incompatible with detection of protons

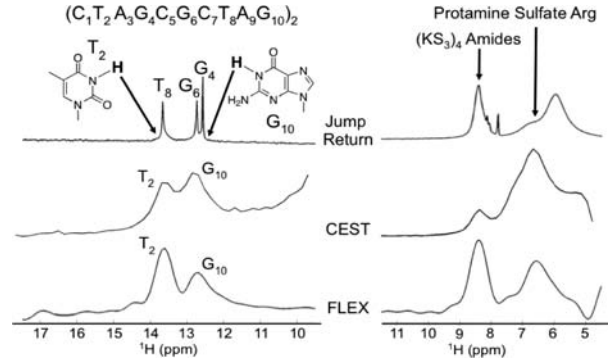

Figure 2. Comparison of several methods for the observation of rapidly exchanging protons in DNA and a peptide mixture (see the text): (left) detection of "invisible" guanine and thymine imino protons at the ends of duplex DNA (pH 9, 20 °C); (right) detection of rapidly exchanging amide and side-chain arginine protons of peptides (pH 7.3) at 37 °C.

exchanging faster than ~1000 Hz. The FLEX sampling criteria are based on the fact that the free-induction decay (FID) is gone after a time $t \approx 5/(k + 1/T^*_2)$, allowing only a few milliseconds for t_{evol}. In order to have sufficient signal, we used a short dwell time (25 μs) to encode the early part of the FID, forcing us to go far off-resonance with carrier o1 to avoid water excitation.

The FLEX approach is expected to have applications in both high-resolution NMR spectroscopy and medical imaging. In the left column of Figure 2, the jump−return (JR), CEST, and FLEX spectra for a 4 mM solution of a 10 base pair palindromic DNA duplex are compared. Even though JR water suppression was used to retain exchangeable protons in the conventional spectrum, only resonances of the T_8, G_4, and G_6 imino protons are visible, while signals for the rapidly exchanging T_2 and G_{10} protons cannot be readily discerned. The contrary is true for the CEST and FLEX spectra, in which only these two imino protons are visible, indicating removal of other protons by the exchange-rate filter. The right column of Figure 2 shows JR, CEST, and FLEX spectra of a mixture of protamine sulfate (PS) and the small polypeptide $(LysSer_3)_4$. These peptides are currently being used as CEST contrast agents for in vivo NMR spectroscopy.[9] The amide (8.3 ppm) resonance represents 12 protons of $(LysSer_3)_4$ and 11 protons of PS (three from Ser, four from Pro, two from Gly, and two from Val). PS has 21 arginines, each with a guanidinium side-chain group, for a total of 84 protons (6.6 ppm).

In order to check the theoretical description, we measured the absolute magnitude of the FLEX transfer signals as a fraction of the total water proton signal (S_0 = 110 M) and compared it with the effects theoretically predicted on the basis of the solute concentrations for both the DNA and protein samples (Table 1). The data were analyzed using time-domain fitting (see the Supporting Information), which provided both the amplitude of the effects for the individual components as well as the signal decay rate during the evolution time. The latter was assumed to be exchange-dominated and used to estimate "k_s". The calculated values in Table 1 predict the experimental results very well for the DNA sample, while the results for the protein mixture are less satisfying. We attribute the latter to several causes, most likely a closer proximity to water, thus reducing λ_s, and the presence of multiple components. In the time-domain analysis, we reconstructed one component for the expected amide and amine proton frequencies and deconvolved the water contribution. As the amide components and amines have multiple frequencies and a range of exchange rates, it is less straightforward to interpret the data.

To better check the theory, we prepared a DNA sample for which exchangeable proton resonances were visible in both the JR (Figure

Table 1. Calculation of FLEX Proton Transfer Ratios

	DNA		protein sample	
	imino T_2	imino G_{10}	amide NH	amine NH_2
freq (ppm)	13.6	12.7	8.4	6.6
$[H]_s$ (mM)[a]	8.0	8.0	20.1	22.7
k_s (s^{-1})[b]	310	3300	370	1400
β_s	0.92	1.00	0.89	1.00
λ_s[c]	0.86	0.77	0.34	0.09
T_{1w} (s)[d]	2.33	2.33	4.12	4.12
PTR (calcd)[e]	1.1%	1.1%	1.7%	0.6%
PTR (meas)[f]	0.7%	1.2%	2.7%	3.5%
PTR (M)[f,g]	0.8	1.3	3.0	3.9

[a] Based on compound concentration and mixture components; for the amide, 11 PS and 12 $(LysSer_3)_4$ protons were included. [b] Estimated from the time-domain decay. [c] Calculated from the experimental water excitation profile for a 90_x pulse as the square of profile intensity at frequency. [d] Measured using an inversion recovery experiment with gradient dephasing to remove radiation damping effects during the inversion time, TI, with a predelay of 15 s and 28 time points between TI = 0.25 and 7 s. [e] Calculated using eqs 1−3 with t_{prep} = 5.36 s (DNA) or 4.40 s (protein), minimum t_{exch} = 8 ms (DNA) or 6 ms (protein), evolution increment = 25 μs, and 126 (DNA) or 251 (protein) increments. [f] Measured from the amplitude of the time domain signal. [g] Calculated with respect to the water proton concentration.

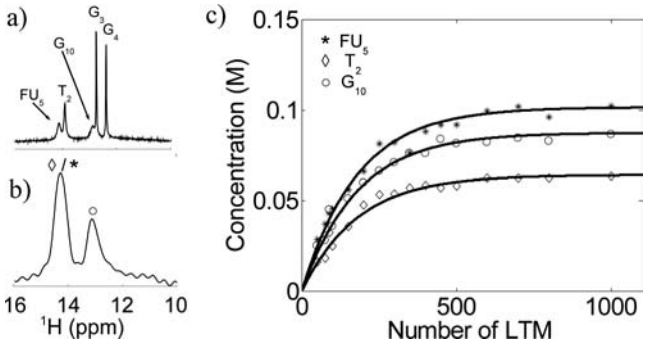

Figure 3. Quantitative validation of the FLEX method for the DNA duplex 5′-$C_1T_2G_3G_4FU_5A_6C_7C_8A_9G_{10}$-3′ ($T$ = 10 °C, pH 9.0). (a) JR spectrum in which all imino protons are observable. (b) FLEX spectra in which G_3 and G_4 do not appear. (c) Concentration of labeled protons generated by FLEX as a function of the number of applied LTMs. The data are based on time-domain fitting, where FU_5 and T_2 could be deconvoluted using prior knowledge of the chemical shift and decay rate. Black lines are best fits of the data to eq 2 (concentration = $PTR_s[H]_w$).

3a) and FLEX (Figure 3b) spectra. Subsequently, we measured the FLEX effect as a function of the number of LTMs. FLEX time-domain fitting was done using the frequencies, decay rates, and exchange rates estimated from the line widths (LWs) (decay rate = $k_s + 1/T_2^* = \pi$LW) in the JR data. The resulting buildup curves for G_{10}, T_2, and fluorouracil (FU_5) were fitted (Figure 3c) to determine the DNA concentration, giving 0.60−0.65 mM (Table 2). This compares satisfactorily to the experimentally determined concentration of 0.8 mM obtained using nucleoside analysis. The excellent correspondence between the experimental and theoretical curve shapes provides further validation of the FLEX method.

In conclusion, we have presented an approach for indirectly detecting signals of multiple rapidly exchanging protons through the water signal while retaining chemical shift specificity and enhancing the sensitivity by factors of 100−200. We expect that these factors can be increased by optimizing the number of LTMs through tuning of the labeling and exchange periods to the exchange rates of particular solute protons. Detection was possible under physiological conditions for rapidly exchanging protons of macromolecules that would otherwise be obscured by a background from more slowly exchanging protons. This editing property of FLEX should be ideally suited to the study of dynamic regions of nucleic acids and proteins where amide, amino, and imino groups move rapidly between a closed solvent-inaccessible state and an exposed state where exchange occurs. Another potential application is enhanced detection of exchange-relayed nuclear Overhauser effects through the water signal, which would require the excitation for the labeling period to include protons in spatial proximity to the exchangeable protons. We expect the FLEX method to have applications in the study of macromolecular structure and interactions (e.g., protein−DNA binding) by high-resolution solution-state NMR spectroscopy as well as in the detection of exchange-based contrast agents for MRI using *frequency transfer* instead of *saturation transfer*. Compared to CEST MRI, FLEX is expected to be less sensitive to B_0 inhomogeneity and interference by slow magnetization transfer processes as a result of the opportunity for time-domain removal of water signals and the capability for exchange rate and frequency filtering, respectively.

Table 2. Fitted and Measured Parameters for the Data in Figure 3

	freq (ppm)	k_s (s^{-1})[a]	β_s	λ_s[b]	$[H]_s$ (mM)[c]
FU_5	14.38	209	0.82	0.58	1.2
T_2	14.16	81	0.49	0.56	1.3
G_{10}	13.14	304	0.92	0.45	1.2

[a] Determined from line widths in the JR spectra corrected for $1/T_2^*$ = 33 Hz based on the width of G_3. [b] Calculated from the experimental water excitation profile for a 90_x pulse as the square of the profile intensity at frequency. [c] From the line fit in Figure 3c (note: $[H]_s$ = 2[DNA]).

Acknowledgment. This work was supported in part by NIH Grants GM056834-14 (J.T.S.) and EB006394 (M.T.M.).

Note Added after ASAP Publication. The Supporting Information was incomplete in the version published ASAP on January 22, 2010; the complete file was posted to the web on January 25, 2010.

Supporting Information Available: Determination of labeling efficiency and details of data analysis procedures. This material is available free of charge via the Internet at http://pubs.acs.org.

References

(1) Gueron, M.; Leroy, J. L. *Methods Enzymol.* **1995**, *261*, 383.
(2) Englander, S.; Kallenbach, N. *Q. Rev. Biophys.* **1983**, *16*, 521.
(3) Cavanagh, J.; Fairbrother, W. J.; Palmer, A. G., III; Skelton, N. J. In *Protein NMR Spectroscopy: Principles and Practice*, 2nd ed.; Elsevier Academic Press: Burlington, MA, 2007.
(4) Ward, K. M.; Aletras, A. H.; Balaban, R. S. *J. Magn. Reson.* **2000**, *143*, 79.
(5) Zhou, J.; van Zijl, P. C. *Prog. NMR Spectrosc.* **2006**, *48*, 109.
(6) Sherry, A. D.; Woods, M. *Annu. Rev. Biomed. Eng.* **2008**, *10*, 391.
(7) Aime, S.; Castelli, D. D.; Crich, S. G.; Gianolio, E.; Terreno, E. *Acc. Chem. Res.* **2009**, *42*, 822.
(8) Ernst, R. R.; Bodenhausen, G.; Wokaun, A. *Principles of Nuclear Magnetic Resonance in One and Two Dimensions*; Oxford University Press: Oxford, U.K., 1990.
(9) McMahon, M. T.; Gilad, A. A.; DeLiso, M. A.; Cromer Berman, S. M.; Bulte, J. W. M.; van Zijl, P. C. M. *Magn. Reson. Med.* **2008**, *60*, 803.

JA909001Q